N.A. GONCHARENKO,[1] O.P. DMYTRENKO,[1] O.L. PAVLENKO,[1] M.P. KULISH,[1]
I.P. PUNDYK,[1] A.I. LESYUK,[1] T.O. BUSKO,[1] A.M. LOPATYNSKYI,[2] V.I. CHEGEL,[2]
V.K. LYTVYN,[2] M.I. KANIUK[3]

[1] Taras Shevchenko National University of Kyiv, Faculty of Physics
  (64/13, Volodymyrs'ka Str., Kyiv 01601, Ukraine; e-mail: poluyannadia@gmail.com)
[2] V.E. Lashkaryov Institute of Semiconductor Physics, Nat. Acad. of Sci. of Ukraine
  (41, Nauky Ave., Kyiv 03028, Ukraine)
[3] O.V. Palladin Institute of Biochemistry, Nat. Acad. of Sci. of Ukraine
  (9, Leontovycha Str., Kyiv 01030, Ukraine)

COMPLEXATION PECULIARITIES IN "DOXORUBICIN–BOVINE SERUM ALBUMIN–GOLD NANOPARTICLES" HETEROSYSTEM. THE FLUORESCENCE STUDY

The fluorescence (FL) quenching in aqueous solutions of doxorubicin (DOX)–bovine serum albumin (BSA)–gold nanoparticles (AuNPs) is studied. The existence of additional mechanisms of DOX-BSA complex formation leading to an increase in the binding constant K and a decrease in the number of binding sites n and the distance between the fluorophore and energy acceptors due to the presence of gold nanoparticles is shown.

K e y w o r d s: doxorubicin, bovine serum albumin, gold nanoparticles, complexation, fluorescence, localized surface plasmon resonance.

1. Introduction

For a long time, anthracycline antibiotics have been successfully used for the anticancer chemotherapy in medical practice. One of their brightest representatives is doxorubicin (DOX) [1, 2]. Like all anthracycline antibiotics, DOX includes a tetrahydrotetracenequinone chromophore molecule consisting of an alicyclic ring and three six-membered complementary aromatic rings. This chromophore is, in turn, bound to the monosaccharide residues and the aglycolic part of the molecule [3–6]. At the same time, the application in clinical practice of anthracycline drugs is limited by the high cardiotoxicity and resistance of tumor cells to these antibiotics. Some tumors are generally not susceptible to anthracycline antibiotics and, therefore, resistant to these drugs [3]. The indicated shortcomings of antibiotics can be partially overcome by the creation of new prodrugs on their

basis with a wider range of influence on tumor cells with reduced resistance, greater selectivity of action only on rebirth cells, with increased latency. To a large extent, the efficacy of prodrugs is also determined by their local delivery to tumors, in which the damage to normal cells is minimized. Such local delivery may be due to a difference in the values of pH of normal and tumor cells which is caused by the hyperbolic activity and the hypotoxic state of the latter [4–6]. Synthesis of prodrugs, including those based on anthracycline antibiotics, is mainly realized by changing the chemical structure of drugs. At the same time, the development of pro-drugs in the form of bioconjugates including molecules of antibiotics and organic or inorganic nanoparticles which can belong to semiconductors or metals, is intensified in recent years. Fullerenes C_{60} and C_{70} are widely used as the organic semiconductor nanoparticles. On the one hand, fullerenes and their water-soluble derivatives can be used to generate singlet-state oxygen in photodynamic therapy and for the inhibition of human immunodeficiency virus, hepatitis C, and DNA strand replication as antioxidants and neuroprotec-

tors. On the other hand, bioconjugates in the form of complexes of molecules C_{60}, C_{70} with antibiotics start to play an important role in anticancer therapy [7–15]. At present, a new direction has been formed in oncology, based on the use of inorganic nanoparticles in molecular diagnostics and therapy of tumor diseases [16–21]. Among inorganic nanoparticles, the most important place in the treatment of various diseases, including oncology, is occupied by the nanostructures of noble metals (gold, silver). The peculiarity of these nanoparticles is the occurrence of the localized surface plasmon resonance (LSPR) phenomenon, while the electromagnetic wave absorption in the visible and near infrared regions of the spectrum takes place in the case where the size of nanoparticles is substantially smaller than the wavelength. The frequency of LSPR oscillations depends on the size and shape of nanoparticles, the distance between them, their location in clusters or aggregates, and on the dielectric properties of the environment [22–31]. The early diagnosis of malignant tumors, determination of their localization, targeted drug delivery to the tumor, and selective (targeted) therapy are possible due to Au and Ag nanoparticles [32]. It should be noted that the creation of stable prodrugs on the basis of bioconjugates with metallic nanoparticles, including gold ones, is associated with difficulties due to their propensity to the aggregation and precipitation in colloidal water solutions. The functionalization of AuNPs, which is aimed at their repulsion due to electrostatic forces, in the case of the production of bioconjugates with prolonged forms of doxorubicin under certain conditions does not provide the stability of molecular systems with AuNPs. In addition, it must be taken into account that one of the priority channels for the delivery of drugs to tumors is their complexation with proteins macromolecules of human or bovine serum albumin (HSA or BSA). The heteroassociation of doxorubicin molecules or functionalized AuNPs with BSA essentially depends on the charge of the protein, which is determined by the pH value [33]. The above-mentioned factors have a combined effect on the complexation mechanisms of DOX-BSA in water solutions. The aim of this work is to determine the effect of gold nanoparticles on the complexation mechanisms of doxorubicin molecules with bovine serum albumin, by using the fluorometry of DOX-BSA-AuNPs aqueous solutions.

2. Preparation of Water Solutions and Techniques of Experiments

In this work, the dosage form of doxorubicin (Teva) in the form of a freeze-dried powder containing 17% active substance and a bovine serum albumin of fraction V for biochemistry (Merck) was used. The colloidal solutions of gold nanoparticles with the mean size of 13 nm obtained as a result of the citrate reduction of tetrachloroauric acid ($C_{Au} = 0.5$ nM) were used as plasmon-producing structures. Deionized water was titrated to pH 7, by using a concentrated NaOH solution. The measurement of fluorescence spectra of doxorubicin solutions with BSA and colloidal gold nanoparticles was carried out on a portable fluorometer "Fluorotest Nano" (ISP NASU) with the excitation at a wavelength of 532 nm.

3. Results and Discussion

The study of the interaction of drug molecules with serum albumin is very important, since this protein is a significant part of blood plasma. More than 60% of this protein are in the system of its circulation and, therefore, play a significant role in the preservation and transport of drugs due to their affinity. At the same time, the mechanisms of affinity and complex formation between macromolecules of proteins and molecules of medical preparations, especially in the presence of metal nanoparticles, are insufficiently studied. This situation is primarily due to the complexity of systems and a significant set of specific interactions during their electron-conformational reorganization in the process of association [34–37]. The fluorescence method can be used to study the characteristics of the DOX-BSA binding, since the structures of DOX and BSA imply the possibility of the emission of these molecules in the relaxation of elementary excitations [38–42]. In addition, the fluorescence bands are substantially spaced apart in the spectral range of wavelengths. Obviously, in the case of DOX-BSA heteroassociation, the photoluminescence extinction [43, 44] can be expected due to the transfer of energy between components. The FL quenching study is performed for doxorubicin in aqueous solutions with a constant concentration of 8.85×10^{-5} M with increase in the BSA content from 0 M to 8.85×10^{-5} M. The fluorescence spectra for DOX-BSA solutions in water are illustrated in Fig. 1. It is seen that the profile of the FL band for
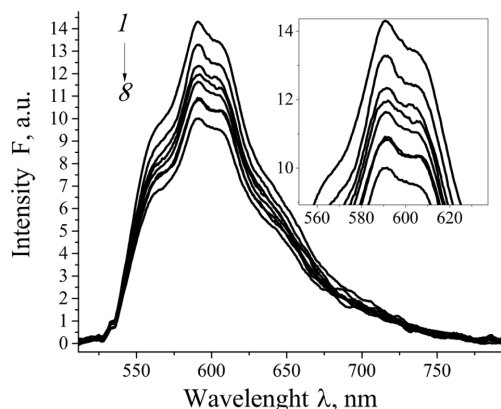
Fig. 1. Fluorescence spectra of DOX-BSA solutions in water at the constant concentration of DOX $C_{DOX} = 8.85 \times 10^{-5}$ M and the variable BSA content The insert shows the FL spectra in the region near the maximum of the band for DOX, $\lambda_{ex} = 532$ nm, $T = 250$ ms, pH $= 7$
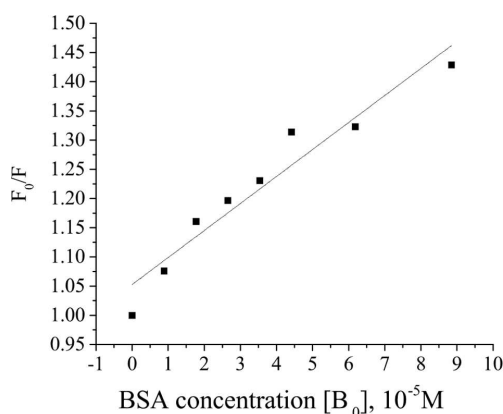

Fig. 2. Representation of the Stern–Volmer FL quenching in a DOX-BSA aqueous solution

doxorubicin is combined of several peaks, the most intense one is located at 594 nm. With the addition of BSA, the FL quenching increases, by retaining the band shape.

The analysis of the FL quenching in the maximum of the band allows us to determine the quenching rate constant K_q, whose value depends, in turn, on the interaction mechanism of the quencher and the fluorophore molecules. In accordance to the Stern–Volmer theory, the static and dynamic mechanisms of such interaction are considered. The predominant influence of one or another mechanism depends on the temperature of a solution. In this case, the maximum value of K_q in the case of dynamic colli-

sions of molecules can reach the magnitude $2.0 \times \times 10^{10}$ s^{-1}M^{-1}. The greater K_q values indicate that, in the solution at this temperature, the static mechanism of interaction by means of the complexation under the action of electrostatic, hydrophobic, hydrogen, and other specific forces is predominantly realized [43, 44].

To determine the K_q quenching constant, we use the Stern–Volmer equation

$$\frac{F_0}{F} = 1 + K_q\tau\,[B_0], \tag{1}$$

where F_0 and F are the fluorescence intensities for DOX solutions at the maximum of the FL band of the drug in the absence and in the presence of the BSA protein macromolecules, respectively, τ_0 is the average lifetime of the fluorophore molecules in the absence of a quencher molecule (for DOX molecules, this value is equal to 6 ns [44]), $[B_0]$ is the concentration of the quencher. On the other hand, it is known that $K_q\tau_0 = K_{SV}$, where K_{SV} is the Stern–Volmer FL quenching constant. Taking the given relation into account, the Stern–Volmer equation can be written as follows:

$$\frac{F_0}{F} = 1 + K_{SV}\,[B_0]. \tag{2}$$

To determine K_{SV}, the dependence F_0 on $[B_0] = C_{BSA}$ is graphically constructed and is approximated by the linear Stern–Volmer equation. Figure 2 shows the representation of the Stern–Volmer FL quenching for a DOX-BSA aqueous solution.

The slope of the approximating line determines the value of the Stern–Volmer constant K_{SV}, which is 4.64×10^3 M^{-1}. For this K_{SV} value, the bimolecular rate constant $K_q = 3.7 \times 10^{12}$ M^{-1}s^{-1}. It exceeds the maximum value of this constant in the case of a dynamic mechanism of interaction between molecules by several orders. This suggests the static association mechanism for the DOX-BSA system. For such complexes, we can determine the affinity constant K_A and the number of binding sites, by using the modified Stern–Volmer equation

$$\frac{F_0 - F}{F} = K_A + [B_0]^n, \tag{3}$$

where K_A is the affinity constant, and n is the number of binding sites. To determine the affinity constant,

the logarithm of the same equation (Hill dependence) can be used:

$$\lg \frac{F_0 - F}{F} = \lg K_A + n \lg [B_0]. \tag{4}$$

Figure 3 shows the dependence of the FL intensity relative change at the band maximum for pure DOX vs the concentration of BSA $B_0 = C_{BSA}$, due to the fluorescence quenching of DOX by protein macromolecules, indicating the DOX-BSA complexation.

The affinity constant $K_A = 2.5 \times 10^{-3}$ M^{-1} obtained after analyzing the graph in Fig. 3 for the DOX-BSA system indicates a high binding affinity of the protein to the drug [44]. In addition, the Hill dependence analysis allows us to obtain the number of binding sites $n = 0.73$ as the slope of the line describing the dependence. Similar calculations can be made, by using another Stern–Volmer equation [35]:

$$\frac{F_0}{F_0 - F} = \frac{1}{fK[B_0]} + \frac{1}{f}, \tag{5}$$

where f is the fraction FL factor, which is introduced by a fluorophore, and K is the complexation constant. The dependence $\frac{F_0}{F_0-F}$ of $\frac{1}{B_0}$ is shown in Fig. 4.

The analysis of the Stern–Volmer dependence shows that $K = 2.01 \times 10^4$ M^{-1} and $f \approx 0.48$.

It is worth mentioning that, in the presence of gold nanoparticles, the FL spectra of DOX and DOX-BSA, while retaining the main features, are more complicated in comparison with spectra without AuNPs. In the presence of AuNPs, a significant decrease in the FL signal intensity is observed in the first hour for a system without BSA (Fig. 5).

The Stern–Volmer quenching constant for the DOX-BSA-AuNPs system calculated according to the graphs (Fig. 7) using Eq. (1) is $K_{SV} = 1.69 \times 10^4$ M^{-1}, which is three times more than the value for the DOX-BSA system. After three days of the exposure of DOX-BSA solutions with nanoparticles, the constant becomes $K_D = 0.56 \times 10^4$ M^{-1}. It can be assumed that changes in the temporal characteristics of the quenching occurring in the ternary system are associated with a decrease in the active surface of AuNPs, which is involved in the energy exchange during the photon capture, as a result of the adsorption of BSA and DOX molecules during the storage time of solutions. The stability of the system was evaluated by measuring the fluorescence characteristics of
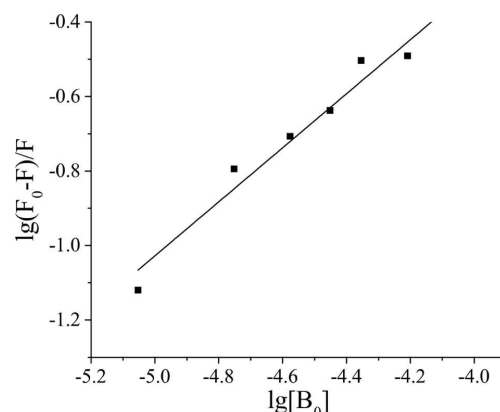

Fig. 3. Hill dependence for DOX-BSA aqueous solutions
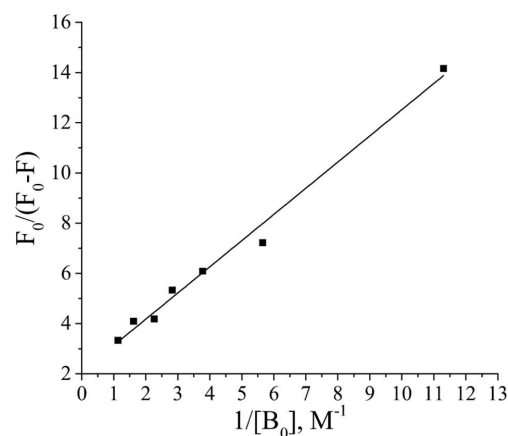

Fig. 4. Stern–Volmer dependence for DOX-BSA aqueous solutions

the DOX-BSA-AuNPs system at the beginning and after three days of exposure (Fig. 6, *a, b*).

In the case of a nanoparticle system, the value of K increases from 0.2×10^5 M^{-1} (without AuNPs) to $K = 7.2 \times 10^5$ M^{-1}, and after a three-day aging of the solution with AuNPs, the value of the constant decreases again to $K = 1.9 \times 10^5$ M^{-1}, which is still an order of magnitude higher than the DOX-BSA value. Therefore, we can conclude that, in the presence of AuNPs, the complexes of different stoichiometries are formed. When gold nanoparticles were added to DOX-BSA solutions, the affinity constant K_A and the number of binding sites n changed significantly (Fig. 7, *a, b*).

It is seen that the values of the affinity constant and the number of binding sites for DOX-BSA-AuNPs solutions obtained immediately after the preparation
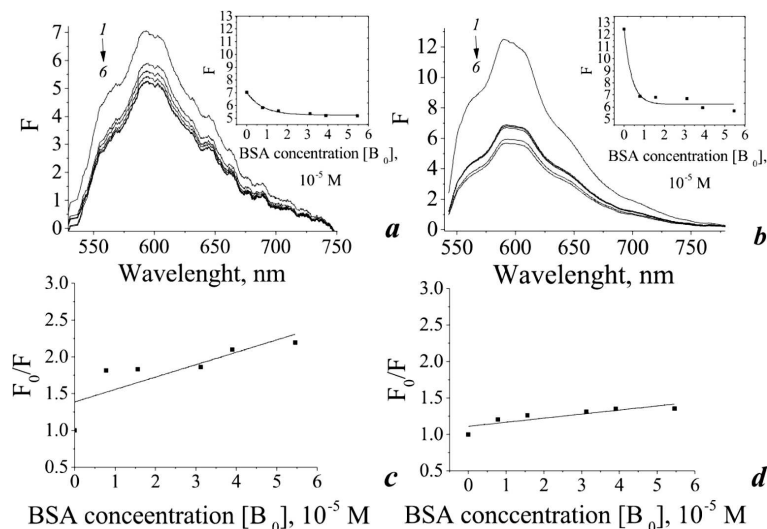
Fig. 5. *a, b* – fluorescence spectra and *c, d* – Stern–Volmer dependences of DOX-BSA-AuNP water solutions of $C_{DOX} = 7.81 \times 10^{-5}$ M , $C_{AuNPs} = 0.31 \times 10^{-9}$ M and the variable content of BSA $[B_0]$ 0 M (*1*), 0.781×10^{-5} M (*2*), 1.56×10^{-5} M (*3*), 3.12×10^{-5} M (*4*), 3.9×10^{-5} M (*5*), and 5.46×10^{-5} M (*6*) obtained directly (*a, c*) and 3 days after samples preparing (*b, d*) (in inserts: FL intensity dependence on the BSA concentration $[B_0]$ near the DOX fluorescence maximum, $\lambda_{ex} = 532$ nm, $t = 25$ °C)
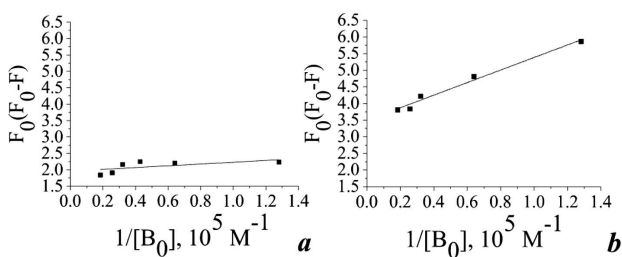

Fig. 6. Modified Stern–Volmer dependences of DOX-BSA-AuNP aqueous solutions obtained directly (*a*) and 3 days after (*b*) the preparation of samples
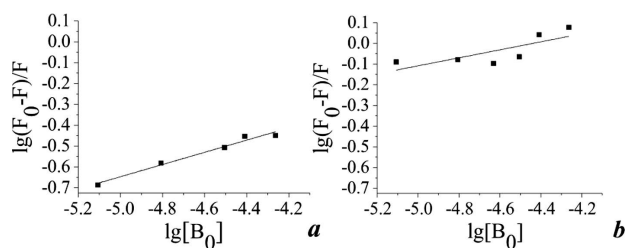

Fig. 7. Hill dependences for DOX-BSA-AuNPs aqueous solutions with variable BSA concentration measured immediately after the preparation of samples (*a*) and after three days of incubation (*b*)

of samples ($K_A = 0.4 \times 10^3$ M^{-1} and $n = 0.725$) are significantly reduced in comparison to similar parameters for DOX-BSA solutions ($K_A = 6.6$ M^{-1}, $n = 0.29 \pm 0.03$). The reason is the simultaneous processes of binding of DOX and BSA molecules, binding of DOX and BSA with AuNPs, as well as binding of BSA with DOX-AuNPs conjuates, which, respectively, causes a significant decrease in the values of K_A and n directly for the DOX-BSA complex. For the FL spectra of DOX-BSA-AuNPs solutions measured after 3 days $K_A = 7.2$ M^{-1}, $n = 0.19 \pm 0.08$. If the initial solutions have a significant decrease in K_A compared with DOX-BSA solutions from 3.95×10^2 M^{-1} to 6.6 M^{-1}, after the exposure for 3 days, the affinity constant increases slightly to 7.2 M^{-1}.

It is worth saying that the proposed method for calculating the constants K and n does not allow one to establish a decrease in the number of free DOX molecules due to the heteroassociation, which is accompanied by the certain Stern–Volmer laws of FL quenching. It is known that the quenching of FL, which is realized as a non-radiation energy transfer, according to Forster's theory, depends on the degree of overlapping of donor radiation spectra (DOX molecules) and the absorption of acceptors (BSA and Au nanoparticles), the relative orientation of the transition dipoles, and the distance between the donor and the acceptor [43].

The efficiency of the transfer of an energy E from DOX to the BSA and AuNPs is determined by the ratio of the FL intensities:

$$E = 1 - \frac{F}{F_0}. \qquad (6)$$

The F value corresponds to the fluorescence intensity for the DOX-BSA solution at a $1:1$ component concentration ratio. On the other hand, the energy transfer efficiency is related to the distance r_0 between the donor and the acceptor according to the relation:

$$E = \frac{R_0^6}{R_0^6 + r_0^6}, \qquad (7)$$

where R_0 is the characteristic (critical) Förster distance. At a distance R_0 between the donor and the acceptor, the energy transfer efficiency is 50 percents

$$R_0^6 = 8.8 \times 10^{-25} K^2 N^{-4} I, \qquad (8)$$

where K^2 is a factor of the spatial orientation of the donor and the acceptor and the correspondence of the mutual orientation of their transition dipoles, N is the index of medium refraction, I is the overlap integral between the donor emission spectra and the acceptor absorption spectra. The value of I is calculated according to the equation:

$$I = \frac{\Sigma F(\lambda)\,\varepsilon(\lambda)\,\lambda^{-4}}{\Sigma F(\lambda)\,\Delta\lambda}. \qquad (9)$$

The value of Φ corresponds to donor's (DOX) quantum yield in the absence of an acceptor. For the calculation of R_0^6, the following values were chosen in the cases of systems DOX-BSA: $K^2 = 2/3$, $\Phi = 0.15$, $N = 1.35$, $I = 4.01 \times 10^{-15}$ cm^{3}M^{-1}. The value $R_0 = 2.2$ nm for the value $E = 0.2$, and the distance between the components of the heteroassociate $r_0 \approx$ ≈ 2.81 nm. In the presence of gold nanoparticles in the DOX-BSA system, these parameters change to $K^2 = 2/3$, $\Phi = 0.15$, $N = 1.40$, $I = 2.4 \times$ $\times 10^{-14}$ cm^{3}M^{-1}, and, so, $R_0 \approx 1.5$ nm. Accordingly, for $E = 0.35$, $r_0 = 1.95$ nm. It can be seen that there is a decrease in the distance between the donor and the acceptor as a result of the presence of an additional gold nanoparticle acceptor.

Thus, in the triple DOX-BSA-AuNPs system, the complexation process between DOX and BSA is complicated by the simultaneous existence of several mechanisms of this heteroassociation. At the same time, the competing processes are realized through the creation of not only DOX-BSA complexes, but also DOX-AuNPs, BSA-AuNPs, and BSA-(DOX-AuNPs). Their presence substantially affects the values of binding constants K, the number of binding n, and the binding distance r_0. To determine these variables that are capable of describing the complex formation in binary systems, it is necessary to involve new methods for the FL quenching with the use of the quantities K, n, and r_0.

4. Conclusions

The complex formation between molecules of the antitumor antibiotic doxorubicin and the macromolecules of the BSA protein is accompanied by the quenching of FL, which can be described by the Stern–Volmer equation. The introduction of a gold spherical nanoparticle into the DOX-BSA system essentially affects the behavior of quenching FL associated with the simultaneous running of several processes in water solutions of DOX-BSA-AuNPs. In addition to the complexation of DOX-BSA, there is the formation of heteroasociates DOX-AuNPs, BSA-AuNPs, and BSA-(DOX-AuNPs). The presence of such processes is accompanied by an increase in the coupling constant between DOX and BSA, and a decrease in the number of binding sites n and the distance r_0 between the donor and the acceptor.

1. F. Arcamone. *Doxorubicin, Anticancer Antibiotics* (Academic Press, 1981) [ISBN: 9780323139731].
2. K. Krohn. Book review: Anthracycline antibiotics *Angew. Chemie* **95**, 649 (1983).
3. A. Garnier-Suillerot, C. Marbeuf-Gueye, M. Salerno *et al.* Analysis of drug transport kinetics in multidrug-resistant cells: Implications for drug action. *Curr. Med. Chem.* **8**, 51 (2001).
4. C. Monneret. Recent developments in the field of antitumour anthracyclines. *Eur. J. Med. Chem.* **36**, 483 (2001).
5. M.N. Preobrazhenskaya, A.N. Tevyashova, E.N. Olsufyeva *et al.* Second generation drugs-derivatives of natural antitumor anthracycline antibiotics daunorubicin. *J. Med. Sci.* 26, **119** (2006).
6. A.N. Tevyashova. Development of progrugs on the basis of anthracycline antibiotics. *Vestn. MITKhT* **9**, 11 (2014).
7. M.P. Evstigneev, A.S. Buchelnikov, D.P. Voronin *et al.* Complexation of C$_{60}$ fullerene with aromatic drugs. *Chem. Phys. Chem.* **14**, 568 (2013).

8. Y.I. Prylutskyy, M.P. Evstigneev, I.S. Pashkova *et al.* Characterization of C_{60} fullerene complexation with antibiotic doxorubicin. *Phys. Chem. Chem. Phys.* **16**, 23164 (2014).

9. Y.I. Prylutskyy, M.P. Evstigneev, V.V. Cherepanov *et al.* Structural organization of C_{60} fullerene, doxorubicin, and their complex in physiological solution as promising antitumor agents. *J. Nanoparticle Res.* **17**, 45 (2015).

10. R.R. Panchuk, S.V. Prylutska, V.V. Chumak *et al.* Application of C_{60} fullerene-doxorubicin complex for tumor cell treatment in vitro and in vivo. *J. Biomed. Nanotechnol.* **11**, 1139 (2015).

11. Y.I. Prylutskyy, V.V. Cherepanov, M.P. Evstigneev *et al.* Structural self-organization of C_{60} and cisplatin in physiological solution. *Phys. Chem. Chem. Phys.* **17**, 26084 (2015).

12. A.A. Mosunov, I.S. Pashkova, M. Sidorova *et al.* Determination of the equilibrium constant of C_{60} fullerene binding with drug molecules. *Phys. Chem. Chem. Phys.* **19**, 6777 (2017).

13. Y. Prylutskyy, A. Borowik, G. Golunski *et al.* Biophysical characterization of the complexation of C_{60} fullerene with doxorubicin in a prokaryotic model. *Materwiss. Werksttech.* **47**, 92 (2016).

14. Y.I. Prylutskyy, V.V. Cherepanov, V.V. Kostjukov *et al.* Study of the complexation between Landomycin A and C_{60} fullerene in aqueous solution. *RSC Adv.* **6**, 81231 (2016).

15. S. Prylutska, R. Panchuk, G. Golunski *et al.* C_{60} fullerene enhances cisplatin anticancer activity and overcomes tumor cell drug resistance. *Nano Res.* **10**, 652 (2017).

16. B. X. Li. Nano-oncology. *Harvard Sci. Rev. Small Sci.* **19**, 42 (2006).

17. S. Nie, Y. Xing, G. J. Kim *et al.* Nanotechnology applications in cancer. *Annu. Rev. Biomed. Eng.* **9**, 257 (2007).

18. L. Prinzen, R.-J.J.H.M. Miserus, A. Dirksen *et al.* Optical and magnetic resonance imaging of cell death and platelet activation using annexin A5-functionalized quantum dots. *Nano Lett.* **7**, 93 (2007).

19. I.V. Plyuto, A.P. Shpak, A.A. Zaporozhets *et al. Nanomaterials and Nanocomposites in Medicine, Biology, and Ecology* (Naukova Dumka, 2011) (in Russian).

20. V. Orel, A. Romanov, O. Rykhalskyi *et al.* Antitumor effect of superparamagnetic iron oxide nanoparticles conjugated with doxorubicin during magnetic nanotherapy of Lewis Lung carcinoma. *Materwiss. Werksttech.* **47**, 165 (2016).

21. V.V. Turov, Y.I. Prylutskyy, T.V. Krupskaya *et al.* Clustering of hydrochloric acid on the surface of C_{60}/C_{70} fullerite and its composites with nanosilica. *Materwiss. Werksttech.* **47**, 172 (2016).

22. T. Zhu, X. Fu, T. Mu *et al.* pH-dependent adsorption of gold nanoparticles on p-aminothiophenol-modified gold substrates. *Langmuir* **15**, 5197 (1999).

23. D.P. O'Neal, L.R. Hirsch, N.J. Halas *et al.* Photo-thermal tumor ablation in mice using near infrared-absorbing nanoparticles. *Cancer Lett.* **209**, 171 (2004).

24. P.K. Jain, I.H. El-Sayed, M.A. El-Sayed. Au nanoparticles target cancer. *Nano Today* **2**, 18 (2007).

25. X. Liu, M. Atwater, J. Wang *et al.* Extinction coefficient of gold nanoparticles with different sizes and different capping ligands. *Colloids Surfaces B Biointerfaces* **58**, 3 (2007).

26. A.M. Lopatynskyi, O.G. Lopatynska, V.I. Chegel *et al.* Localized surface plasmon resonance biosensor-part I: Theoretical study of sensitivity-extended Mie approach. *IEEE Sens. J.* **11**, 361 (2011).

27. S. Zeng, K.-T. Yong, I. Roy *et al.* A review on functionalized gold nanoparticles for biosensing applications. *Plasmonics* **6**, 491 (2011).

28. A.M. Goodman, Y. Cao, C. Urban *et al.* The surprising in vivo instability of near-IR-absorbing hollow Au–Ag nanoshells. *ACS Nano* **8**, 3222 (2014).

29. A.J. Trouiller, S. Hebie, F. El Bahhaj *et al.* Chemistry for oncotheranostic gold nanoparticles. *Eur. J. Med. Chem.* **99**, 92 (2015).

30. J. Zhu, W. Li, M. Zhu *et al.* Influence of the pH value of a colloidal gold solution on the absorption spectra of an LSPR-assisted sensor. *AIP Adv.* **4**, 1 (2014).

31. M. Xiao, Y.M. Chen, M.N. Biao *et al.* Bio-functionalization of biomedical metals. *Mater. Sci. Eng. C* **70**, 1057 (2017).

32. Yu.P. Meshalkin, N.P. Bgatova. Perspectives and problems of the application of inorganic nanoparticles to oncologggy. *J. Sib. Fed. Univ. Biol.* **3**, 248 (2008).

33. N.A. Goncharenko, O.L. Pavlenko, O.P. Dmytrenko *et al.* Gold nanoparticles as a factor of influence on doxorubicin–bovine serum albumin complex. *Appl. Nanosci.* **9**, 825 (2019).

34. K. Vuignier, J. Schappler, J.-L. Veuthey *et al.* Drug–protein binding: A critical review of analytical tools. *Anal. Bioanal. Chem.* **398**, 53 (2010).

35. J. Pan, Z. Ye, X. Cai *et al.* Biophysical study on the interaction of ceftriaxone sodium with bovine serum albumin using spectroscopic methods. *J.Biochem. Mol. Toxicol.* **26**, 487 (2012).

36. Q. Yue, T. Shen, C. Wang *et al.* Study on the interaction of bovine serum albumin with ceftriaxone and the inhibition effect of zinc (II). *Int. J. Spectrosc.* **1** (2012).

37. J. Wu, R. Wei, H. Wang *et al.* Underlying the mechanism of vancomycin and human serum albumin interaction: A biophysical study. *J. Biochem. Mol. Toxicol.* **27**, n/a (2013).

38. A. Sulkowska. Interaction of drugs with bovine and human serum albumin. *J. Mol. Struct.* **614**, 227 (2002).

39. A. Mallick, S. Maiti, B. Haldar *et al.* Photophysics of 3-acetyl-4-oxo-6,7-dihydro-12H indolo-[2,3-a] quinolizine: Emission from two states. *Chem. Phys. Lett.* **371**, 688 (2003).

40. L. Birla, A. M. Cristian, M. Hillebrand. Absorption and steady state fluorescence study of interaction between eosin

and bovine serum albumin. *Spectrochim. Acta – Part A Mol. Biomol. Spectrosc.* **60**, 551 (2004).

41. L. Trynda-Lemiesz. Paclitaxel-HSA interaction. Binding sites on HSA molecule. *Bioorganic Med. Chem.* **12**, 3269 (2004).

42. S. Deepa, A.K. Mishra. Fluorescence spectroscopic study of serum albumin-bromadiolone interaction: Fluorimetric determination of bromadiolone. *J. Pharm. Biomed. Anal.* **38**, 556 (2005).

43. S. Bi, Y. Sun, C. Qiao *et al.* Binding of several anti-tumor drugs to bovine serum albumin: Fluorescence study. *J. Lumin.* **129**, 541 (2009).

44. D. Agudelo, P. Bourassa, J. Bruneau *et al.* Probing the binding sites of antibiotic drugs doxorubicin and N-(trifluoroacetyl) doxorubicin with human and bovine serum albumins. *PLoS One* **7**, 1 (2012).

Received 02.09.19

Н.А. Гончаренко, О.П. Дмитренко,
О.Л. Павленко, М.П. Куліш, І.П. Пундик,
А.І. Лесюк, Т.О. Буско, А.М. Лопатинський,
В.І. Чегель, В.К. Литвин, М.І. Канюк

ОСОБЛИВОСТІ КОМПЛЕКСОУТВОРЕННЯ
В ГЕТЕРОСИСТЕМІ "ДОКСОРУБІЦИН–БИЧАЧИЙ
СИРОВАТКОВИЙ АЛЬБУМІН-НАНОЧАСТИНКИ
ЗОЛОТА." ДОСЛІДЖЕННЯ ФЛУОРЕСЦЕНЦІЇ

Р е з ю м е

Вивчено гасіння флуоресценції (ФЛ) в розчинах у воді DOX-BSA-AuNPs. Показано, що в присутності наночастинок золота виникають додаткові механізми комплексоутворення, які приводять до зростання константи зв'язування K та падіння числа зв'язуючих місць n і відстані між флуорофором та акцепторами енергії.